JOURNAL OF Materials CHEMISTRY

# Effect of plasticizer and temperature on the photorefractive phase shift in fully functionalized polymethacrylates

**David Van Steenwinckel,*[a] Eric Hendrickx,[a] Celest Samyn,[b] Christiaan Engels[b] and André Persoons[a]**

[a]*Laboratory for Chemical and Biological Dynamics, Center for Research on Molecular Electronics and Photonics, University of Leuven, Celestijnenlaan 200D, B-3001 Leuven, Belgium*
[b]*Laboratory of Macromolecular and Physical Organic Chemistry, University of Leuven, Celestijnenlaan 200F, B-3001 Leuven, Belgium*

***Received 3rd July 2000, Accepted 29th August 2000***
***First published as an Advance Article on the web 10th October 2000***

We have analyzed the evolution of the photorefractive phase shift and the photoconductivity in three fully functionalized photorefractive polymethacrylates with increasing temperature and plasticizer concentration. Apart from a strong increase in refractive index modulation amplitude, the polymers show a larger phase shift and photoconductivity as the measurement temperature is raised. When the measurement temperature is kept at 21 °C, the photorefractive performance can be improved by reducing the glass transition temperature of the polymers by adding an external plasticizer. Two types of plasticizer were used. When doped with 10 or 20 wt% of an inert plasticizer (IP), diffraction efficiencies and gain coefficients are improved substantially. Due to a dilution of the charge transporting groups, however, the photoconductivities and the phase shifts start to decrease when more than 10 wt% of inert plasticizer is added. A detailed analysis of this behaviour is presented. When the carbazole-functionalized copolymers with carbazole as the only charge transporting group are doped with 20 wt% of *N*-ethylcarbazole, the concentration of the charge transport molecules is increased. Together with the lowering of $T_g$, this produces a larger phase shift. In all experiments, a good correlation between photoconductivity and photorefractive phase shift was observed.

## Introduction

The photorefractive effect involves the modulation of the refractive index by a space charge field *via* the Pockels effect and birefringence.[1,2] Photorefractive materials are multifunctional, combining photoconductivity and electro-optic activity. Because of a widespread range of applications, PR materials have received considerable attention over the past few years. Compared to the inorganic crystals, where the photorefractive effect was originally discovered, organic polymers have the advantages of a better processability, lower cost, larger electro-optic coefficients, and lower relative permittivities. Additionally, the extension of the optical wavelength at which charge generation occurs to the near IR region provides compatibility with low-cost laser diodes.[3] The most successful photorefractive materials so far are composites based on the photoconductor poly-(*N*-vinylcarbazole) (PVK), doped with 50 wt% of molecular dopants, such as NLO-chromophores and plasticizer molecules. A disadvantage of these intensely studied composite materials, however, is their tendency towards phase separation.[4,5] Since fully functionalized polymers offer the best perspectives in terms of stability,[6,7] we have synthesized three photorefractive methacrylic copolymers in which the chromophore unit is polymerized along with the charge transporting unit.

In a previous paper, we have presented the synthesis of these fully functionalized photorefractive polymers, and their photorefractive properties at three different temperatures.[8] The polymer structures are shown in Fig. 1a. Briefly, the polymers had a polymethacrylate backbone, and were functionalized with a carbazole group, a plasticizing dodecyl group, and a different nonlinear optical chromophore for each polymer. The compositions, as determined by $^1$H-NMR, and the glass transition temperatures ($T_g$) of the resulting copolymers are shown in Table 1. Doped with 1 wt% of the

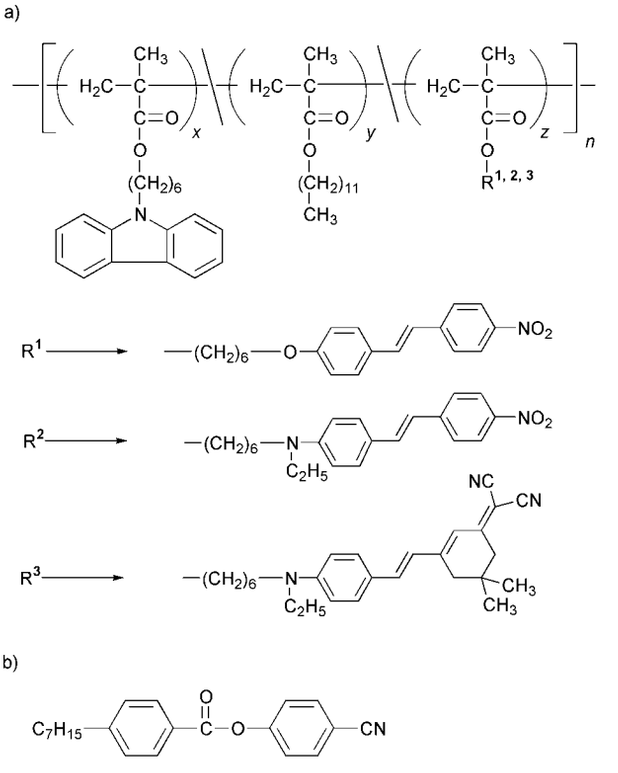


**Fig. 1** a) Chemical structure of the fully functionalized photorefractive polymethacrylates; b) Structure of the liquid crystal used as plasticizer.

 DOI: 10.1039/b005295g

**Table 1** Composition and $T_g$ of the synthesized polymethacrylates

| Polymer | Chromophore [a] | $x/y/z$ [b] | $T_g$/°C [c] |
|---|---|---|---|
| **1** | $R^1$ | 0.45/0.0/0.55 | 66 |
| **2** | $R^2$ | 0.46/0.23/0.31 | 47 |
| **3** | $R^3$ | 0.45/0.18/0.37 | 52 |

[a] The chromophore incorporated in the polymer. The chromophores are shown in Fig. 1. [b] Polymer composition: percentage of carbazole, dodecyl, and chromophore units incorporated in the polymer, as determined by $^1$H-NMR. [c] Determined by DSC measurements, at a scanning rate of 20 °C min$^{-1}$.

sensitizer (2,4,7-trinitrofluoren-9-ylidene)malononitrile (TNFM), all polymers showed good photorefractive properties, although $T_g$ was too high to allow efficient poling of the chromophores at room temperature. As the measurement temperature was raised and approached $T_g$, the photorefractive properties improved significantly, mainly because of the higher rotational mobility of the NLO-chromophores, or the improved contribution of birefringence to the total refractive index modulation.[9] The temperature was controlled by a hot stage in the optical set-up. To eliminate the need for such a hot stage, however, an alternative method to improve the PR properties would be to lower the $T_g$ of the polymer samples, *e.g.* by adding an external plasticizer. After addition of a plasticizer, the chromophores also gain rotational mobility, and the contribution of birefringence is again enhanced. The external plasticizer is present in smaller concentration than the chromophore dopants in traditional composites, and can be selected to have good compatibility with the polymer.

In the more fundamental study presented in this paper, both pathways for improving the photorefractive performance, and their effect on the photoconductivity and the photorefractive phase shift, are examined closely. In a first section, the evolution of the refractive index modulation amplitude upon doping the polymers with an external plasticizer is discussed. In a second section, the effect of a temperature increase on the photorefractive phase shifts in the samples containing only the functionalized polymers and the sensitizer TNFM is investigated. It is well accepted that the refractive index modulation and the gain coefficient are enhanced as the chromophores gain rotational mobility, but an evolution of the PR phase shift as the sample is scanned through its glass transition temperature has not been reported yet. The correlation between the phase shift and the photoconductivity is also discussed. In section III, we analyze the phase shift evolution in samples containing the polymers, TNFM, and different concentrations of an external plasticizer at a constant temperature. Having tested two types of plasticizer (inert and charge transporting plasticizers), we present an evaluation of which one is the better plasticizer. Finally, we compare the evolution of the phase shift in sections II and III.

## Results and discussion

### I. Evolution of the refractive index modulation upon plasticizing

Small amounts of plasticizer (10–20 wt%) were added to the fully functionalized polymethacrylates to lower the glass transition temperature, and to enhance the rotational flexibility of the functional groups. To avoid scattering and bad fringe contrasts as a consequence of phase separation, the plasticizer must be highly compatible with the host polymer. We have synthesized the liquid crystal (LC), shown in Fig. 1b, and have used it as a plasticizer. The pure liquid crystal shows a nematic phase between 42 and 53 °C. Upon cooling, the transition from the isotropic to the nematic state occurs at 53 °C, but the crystalline phase is only recovered at 10 °C. When dissolved in the polymer matrix, however, no mesophase was observed. Hence, it should be emphasized that the liquid crystal in these samples is uniformly dissolved in the polymer, unlike in polymer dispersed liquid crystals (PDLCs), where a phase separation between the LC chromophores and the polymer matrix is induced by cooling down rapidly.[10] In a PDLC, the LC chromophores reorient co-operatively at low electric fields because of the high rotational mobility of liquid crystals. As a consequence, application of an electric field aligns the LC droplets in the polymer binder, and reduces scattering in the sample. This results in an increase in transmittance for the PDLCs. Although we have been able, using other polymers, to prepare PDLCs with the LC in Fig. 1b, doping the present polymers (in Fig. 1a) with 20 wt% LC did not lead to the formation of PDLCs. In the samples discussed in this paper, phase separation of the liquid crystal has not occurred at ambient temperature since the preparation of the first samples (>10 months). An increase in transmittance upon application of an electric field was not observed, neither was there an indication of a mesophase in DSC experiments. This confirms that the critical concentration for phase separation is not achieved in these samples, and that the plasticizer is dissolved uniformly in the polymer matrix. Nevertheless, the liquid crystal molecules are accompanied by a large free volume, which is evidenced by a large decrease in $T_g$ when dispersed in the polymer matrix, and a larger contribution of birefringence to the total refractive index modulation.[9] The LC, having a nonzero polarizability anisotropy and dipole moment, also improves the total refractive index modulation through its photorefractive figure of merit. Taking into account the dipole moment, the polarizability anisotropy, and the number density of the LC in the samples, the contribution of the LC can amount to 25% of the total refractive index modulation. Yet, the LC plasticizer has no hole-transporting properties, neither does it form a charge-transfer complex with *N*-ethylcarbazole, the chromophores, or TNFM. Hence, when doped with LC, the charge transporting properties of the polymers are only affected through dilution of the charge transporting moieties in the mixture. Since this paper focuses on the behaviour of the phase shift, and hence on the transport of the charges rather than the magnitude of the refractive index modulation, the liquid crystal in this paper is referred to as an inert plasticizer (IP).

If 10 or 20 wt% of the LC plasticizer (IP) is dissolved in the polymer matrix, the $T_g$ is lowered by 20 to 40 °C, and the diffraction efficiency of the samples at room temperature (21 °C) is significantly improved. Diffraction efficiencies of polymers **1**, **2**, and **3**, doped with 0, 10, or 20 wt% IP, are shown in Fig. 2a, b, and c, respectively. All samples contained 1 wt% of TNFM-sensitizer, and the experimental wavelength was 780 nm. As mentioned above, the large improvements in diffraction efficiency after doping with IP are due to the higher rotational mobility of the chromophore groups, producing a larger contribution of birefingence to the total refractive index modulation,[9] and due to a contribution of the IP itself. The relation between the refractive index modulation amplitude $\Delta n$ and the internal diffraction efficiency $\eta$ is:

$$\eta = \sin^2(564\Delta n) \quad (1)$$

Eqn. (1) was obtained from the coupled wave theory for thick holograms developed by Kogelnik, after filling in all geometry factors of the optical setup.[11]

A similar increase in diffraction efficiency has been observed for the pure copolymers with increasing temperature.[8] At higher temperatures, the chromophores also gain rotational mobility. However, the increase in temperature for a fully functionalized polymer is not equivalent to reducing the $T_g$ by adding a plasticizer. Being unable to transport charges, the plasticizer affects the charge transporting characteristics of the polymers through the dilution of the charge transporting

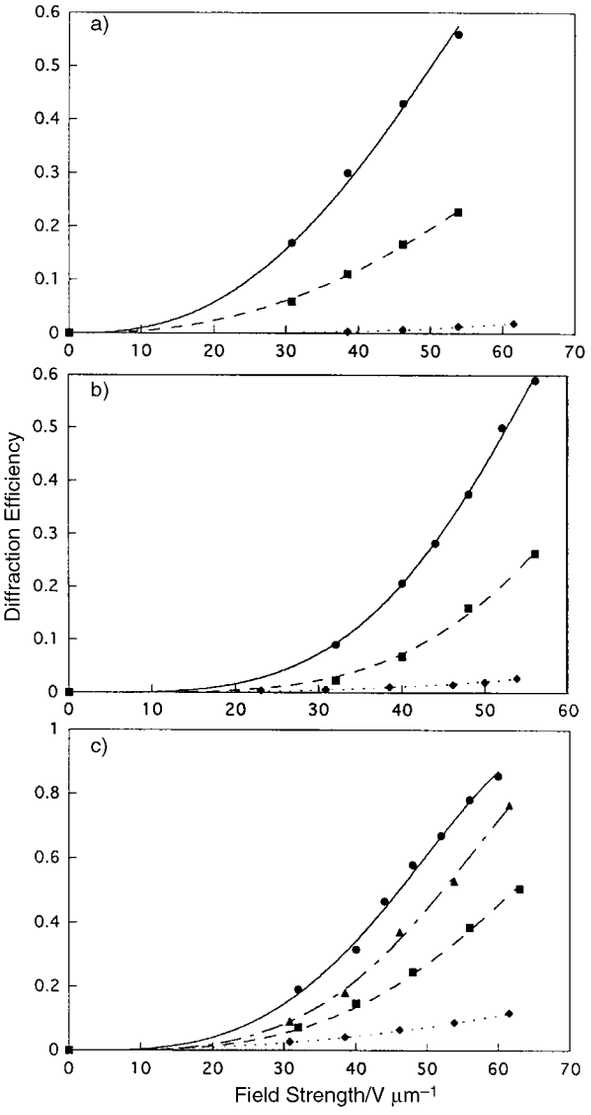


**Fig. 2** a) Internal diffraction efficiencies for polymer **1**, doped with 0 (◆), 10 (■), and 20 wt% (●) of IP *versus* applied electric field; b) Internal diffraction efficiencies for polymer **2**, doped with 0 (◆), 10 (■), and 20 wt% (●) of IP *versus* applied electric field; c) Internal diffraction efficiencies for polymer **3**, doped with 0 (◆), 10 (■), and 20 wt% (●) of IP, and (▲) a sample of polymer **3**, plasticized with 20 wt% of *N*-ethylcarbazole, *versus* applied electric field. The lines are fits of the diffraction efficiency according to Kogelnik's coupled wave theory for thick transmission gratings.

groups. Thus, even if the pure copolymer and the plasticized copolymer are at the same temperature with respect to their $T_g$, the photorefractive properties can be different. Therefore, in the remainder of the discussion, we analyze the photoconductivity and the photorefractive phase shift.

## II. Phase shift evolution with increasing measurement temperature

Using eqn. (1), refractive index modulation amplitudes $\Delta n$ can be calculated from the measured diffraction efficiencies. If the two-beam coupling gain coefficients $\Gamma$ are measured as well, the photorefractive phase shifts can be calculated using eqns. (1) and (2):

$$\Gamma = \frac{4\pi}{\lambda}(\hat{e}_1\hat{e}_2^*)\Delta n \sin\vartheta \qquad (2)$$

where $\lambda$ is the optical wavelength, $\hat{e}_1$ and $\hat{e}_2$ are the polarization vectors of the two writing beams, and $\vartheta$ is the phase shift between the space-charge field and the interference pattern generated by the interacting beams.[1] The PR phase shift slightly increases with the applied electric field. Diffraction efficiencies and gain coefficients for the three copolymers without plasticizer at 48 V μm$^{-1}$ were measured at three different temperatures.[8] The two upper temperatures for each polymer were chosen to perform the PR measurements at the same distances from $T_g$, to minimize the differences in the contributions of birefringence to the total refractive index modulation amplitude. It is important to note that the diffraction efficiencies and the gain coefficients were allowed to reach steady state values. For polymers **2** and **3**, the grating build-up was complete after 1 minute, while polymer **1** needed 5 minutes. Therefore, the values for the phase shifts at 48 V μm$^{-1}$ and at three different temperatures, which are shown in Table 2, were obtained from diffraction efficiencies and gain coefficients after 5 minutes of grating formation at 48 V μm$^{-1}$.

As can be seen from Table 2, the photorefractive phase shift is largely enhanced with increasing measurement temperature in all polymers. The phase shift measured in a photorefractive experiment is a good measure of the mean distance the photogenerated holes can migrate from the light intensity maximum, where they are generated. Thus, it can be expected that the magnitude of the phase shift correlates with the mobility of the charges, that is, the ability of the photogenerated holes to hop from one charge transporting unit to another. To study the correlation between charge mobility and the photorefractive phase shifts, we have measured the photoconductivity at a field of 48 V μm$^{-1}$, and at the three temperatures where the PR measurements were performed. The photoconductivity of a polymer is proportional to the photogeneration efficiency and the mobility of the charges.[12] Photoconductivities were obtained by measuring the voltage change over a resistor (resistance $R = 1$ MΩ) in series with a biased (applied field $E = 48$ V μm$^{-1}$) sample, when it was illuminated with a 200 ms light pulse ($\lambda = 780$ nm, irradiance = 130 mW cm$^{-2}$). For polymer **1**, no reliable photoconductivity data could be obtained, because of a low signal-to-noise ratio. For polymers **2** and **3**, however, the data were highly reproducible (5%). As can be seen in Table 2, when the temperature of the polymer mixture is raised and approaches $T_g$, the photoconductivity of the samples increases. Hence, for polymers **2** and **3**, the proportionality between the photoconductivity and the phase shift is clear: both increase with temperature. An increase in phase shift with temperature was also observed in polymer **1**. At this point, it is not clear yet whether it is the photogeneration efficiency or the charge mobility (both increasing with temperature) which is responsible for the higher PR phase shift. This will be the subject of a further study.

The larger photoconductivities at higher temperatures,

**Table 2** Photoconductivities and photorefractive phase shifts at different temperatures in the copolymers without plasticizer

| Polymer | $T_e$/°C [a] | $T_e - T_g$/°C [b] | $\sigma_{ph}$/pS cm$^{-1}$ [c] | $\vartheta$/° [d] |
|---|---|---|---|---|
| **1** | 21 | −45 | — | 4.1 |
| **1** | 50 | −16 | — | 9.5 |
| **1** | 68 | +2 | — | 11.5 |
| **2** | 21 | −26 | 0.15 | 6.2 |
| **2** | 31 | −16 | 0.20 | 8.0 |
| **2** | 49 | +2 | 0.23 | 13.0 |
| **3** | 21 | −31 | 0.19 | 6.0 |
| **3** | 36 | −16 | 0.22 | 8.1 |
| **3** | 54 | +2 | 0.26 | 13.2 |

[a] $T_e$ is the temperature at which the experiment was performed. [b] $T_g$ is the glass transition temperature of the polymer, determined by differential scanning calorimetry, at a heating rate of 20 °C min$^{-1}$. [c] $\sigma_{ph}$ is the photoconductivity, measured at 48 V μm$^{-1}$, 780 nm and a light intensity of 130 mW cm$^{-2}$. [d] $\vartheta$ is the photorefractive phase shift, calculated from diffraction efficiencies and gain coefficients, using eqns. (1) and (2), at an applied field of 48 V μm$^{-1}$.

which correlate with the larger phase shifts, are partly the consequence of higher charge mobilities. These can be attributed to the destruction of conformational traps in the carbazole-based copolymer by the micro-Brownian motion of the polymer chains in the glass transition region.[13,14] Above a certain temperature, the trap level of this conformational trap becomes shallow. It has been argued that the activation energy term in the drift mobility is in part the consequence of a site's variable local potential.[15] The disorder induced potential could be influenced by the onset of a dynamic process as chain motion, characteristic for the glass transition region. It is important to note that the largest activation energy for the mobility is found in the temperature region below $T_g$. Around and above $T_g$ a smaller activation energy was observed. This confirms that, as was mentioned above, the trap level of the conformational trap becomes shallow at a certain temperature. An Arrhenius plot of log (photoconductivity) *versus* 1000/$T$ of polymer **3** is shown in Fig. 3. The fact that we observe a change in the slope of the log (photoconductivity) in Fig. 3 at a certain temperature, similar to what has been observed in mobility experiments,[15] indicates that the photoconductivity in these samples is a good measure of the charge mobility.

Another study, by Slowik and Chen, has also argued that the mobility increases as the carbazole moieties gain rotational mobility, due to a better overlap between adjacent carbazole groups.[16] In conclusion, when the temperature is raised, the mobilities, and hence also the photoconductivities and the phase shifts, increase.

### III. Phase shift evolution upon plasticizing

**a. Doping with an inert plasticizer (IP).** If the inert plasticizer (IP) is added to the copolymers, the situation is more complex. In Fig. 4a, b, and c, we can see that, apart from the diffraction efficiencies (Fig. 2), the gain coefficients are also strongly enhanced upon addition of plasticizer. This was expected, from the direct proportionality between the gain coefficient and the refractive index modulation amplitude (eqn. (2)). When Fig. 4 is examined closely, however, it is clear that mixtures with 10 wt% IP (■) have gain coefficients relatively close to the gain coefficients of mixtures with 20 wt% IP (●), while the diffraction efficiencies, in Fig. 2, differ substantially. From eqn. (2), this implies that samples with 10 wt% IP must have a higher photorefractive phase shift than samples containing 20 wt% IP. Phase shifts for the samples with different concentrations of IP, at 48 V $\mu m^{-1}$, have been calculated in the same manner as explained in the previous section, and the results are shown in Table 3. These results clearly show that, for all polymers, adding 10 wt% IP enlarges the photorefractive phase shift, whereas the phase shift decreases after addition of 20 wt% IP.

In Fig. 5, the phase shifts of polymer **2** are plotted *versus* the difference between the experimental temperature and $T_g$, for two different experimental approaches. Fig. 5 points out that, as was anticipated, reducing the $T_g$ by adding an inert plasticizer is not equivalent to a temperature increase for the pure copolymers. An increase in measurement temperature always induces a larger phase shift (circles, solid line, see also Table 2). Adding a plasticizer also reduces the difference between the experimental temperature and $T_g$, but leads to a maximum in the phase shift evolution (triangles, dashed line).

Using the same rationale as above, we can say that adding 10 wt% IP lowers $T_g$ and improves the rotational mobility of the functional groups in the copolymer. Consequently, more conformational traps are destroyed, and a better overlap between adjacent carbazoles is possible, which enlarges the charge mobility.[14,16] As shown in Table 3, both the photoconductivities and phase shifts increase upon addition of 10 wt% IP. If more (20 wt%) plasticizer is added, the photoconductivity and phase shift decrease. This is not obvious, since the increase in plasticizer concentration further lowers $T_g$ and should raise the mobility again. However, an

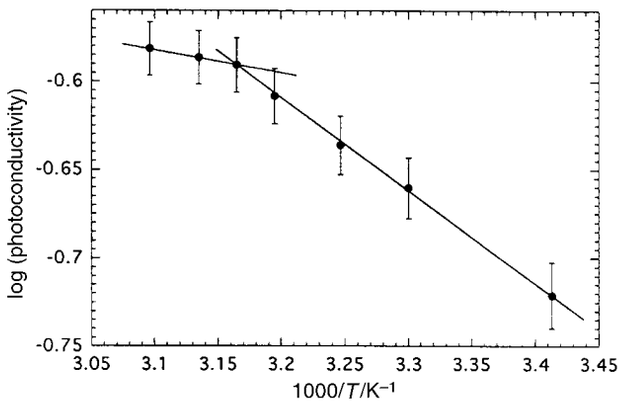


**Fig. 3** Arrhenius plot of log (photoconductivity) *versus* 1000/$T$ for polymer **3**. The lines are guides to the eye.

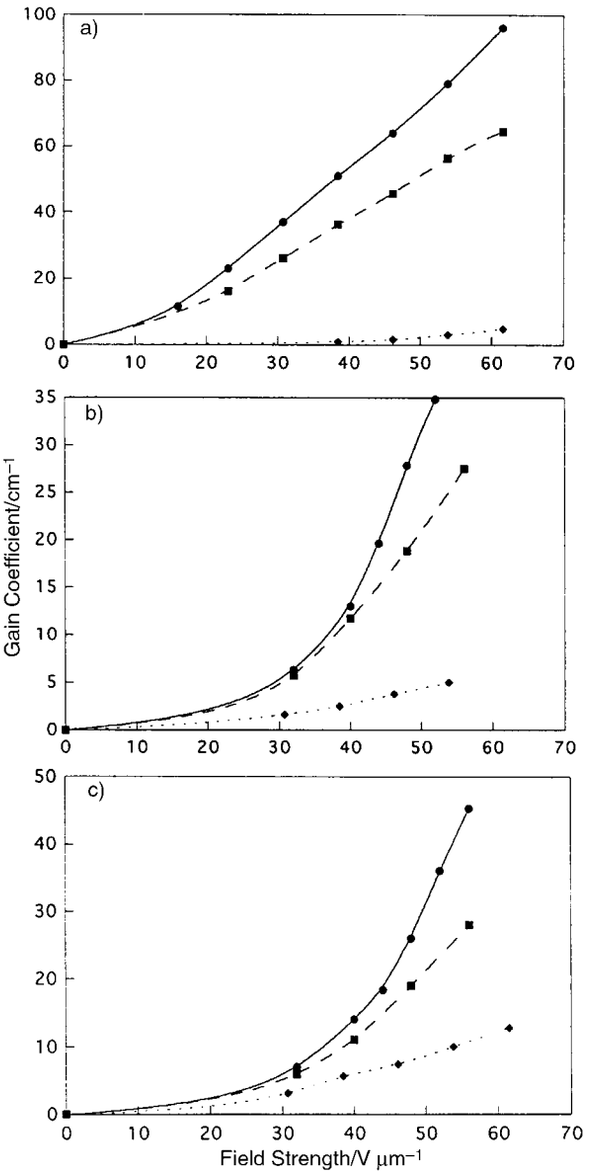


**Fig. 4** a) Gain coefficients for polymer **1**, doped with 0 (◆), 10 (■), and 20 wt% (●) of IP *versus* applied electric field; b) Gain coefficients for polymer **2**, doped with 0 (◆), 10 (■), and 20 wt% (●) of IP *versus* applied electric field; c) Gain coefficients for polymer **3**, doped with 0 (◆), 10 (■), and 20 wt% (●) of IP *versus* applied electric field. The lines are guides to the eye.

**Table 3** Photoconductivities and photorefractive phase shifts at 21 °C in samples containing 0, 10 and 20 wt% of inert plasticizer

| Polymer | IP concentration (wt%) | $T_g$/°C [a] | $\sigma_{ph}$/pS cm$^{-1}$ [b] | $\vartheta$/° [c] |
|---|---|---|---|---|
| **1** | 0 | 66 | — | 4.1 |
| **1** | 10 | 38 | — | 21.2 |
| **1** | 20 | 15 | — | 18.4 |
| **1** | 20 wt% ECZ | 32 | — | 26.2 |
| **2** | 0 | 47 | 0.15 | 6.2 |
| **2** | 10 | 30 | 0.22 | 9.3 |
| **2** | 20 | 10 | 0.19 | 8.2 |
| **3** | 0 | 52 | 0.19 | 6.0 |
| **3** | 10 | 33 | 0.28 | 8.2 |
| **3** | 20 | 14 | 0.25 | 7.1 |

[a] $T_g$ is the glass transition temperature of the polymer mixture, determined by differential scanning calorimetry, at a heating rate of 20 °C min$^{-1}$. [b] $\sigma_{ph}$ is the photoconductivity, measured at 48 V μm$^{-1}$, 780 nm and a light intensity of 130 mW cm$^{-2}$. [c] $\vartheta$ is the photorefractive phase shift, calculated from diffraction efficiencies and gain coefficients, using eqns. (1) and (2), at an applied field of 48 V μm$^{-1}$.

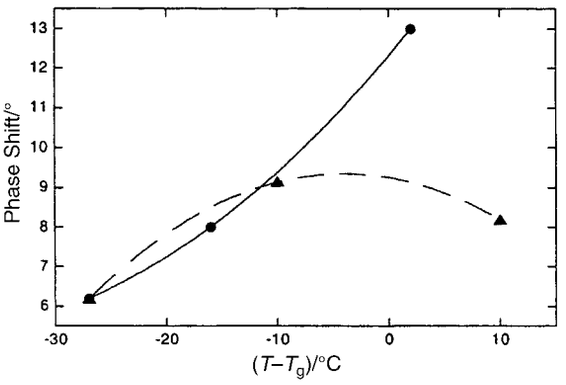


**Fig. 5** Evolution of the phase shift as a function of the difference between the experimental temperature and $T_g$ in polymer **2**. (●): Approaching $T_g$ by means of heating the sample; (▲): Approaching $T_g$ by lowering the $T_g$ value itself, and keeping the measurement temperature constant. The lines are guides to the eye.

increase in plasticizer concentration also implies a lower concentration of charge transport moieties. Hence, it is more difficult for the holes to find an adjacent charge transporting group, which results in lower mobility and photoconductivity. Thus, in conclusion, there are two competing effects. The evolution of the photoconductivity upon doping the polymer samples with IP will be determined by the largest effect.

Addition of the first 10 wt% IP lowers the $T_g$ of the polymers from around 50 °C to $T_g$ values close to 30 °C (see Table 3). When measured at 21 °C, the motion of the pendant carbazole groups, on the time scale of several minutes, is much less restricted compared to when the $T_g$ is 50 °C. Hence, a better approach between the adjacent carbazole moieties is possible, which enhances the mobility and makes it easier for the holes to migrate towards the darker parts of the illumination pattern. At these small IP concentrations, the dilution of the charge transporting molecules appears to be less important than the large enhancement in photoconductivity, which originates in a larger orientational mobility of the functional groups.

Increasing the IP concentration up to 20 wt% reduces $T_g$ to temperatures around 15 °C. This lowering of the $T_g$ below the measurement temperature (21 °C) implies the introduction of an additional free volume, and a higher orientational flexibility for the functional groups. The gain in orientational flexibility at this stage, however, is much smaller than the gain in orientational flexibility upon addition of the first 10 wt% IP. To verify this experimentally, we have studied the orientational flexibility of the pendant chromophores, by calculating the refractive index modulations of the different samples at 48 V μm$^{-1}$ from the diffraction efficiencies, using eqn. (1). The photorefractive index modulation consists of an electro-optic and a birefingence contribution.[9] The latter is dependent on the orientational flexibility of the chromophores. Calculating the ratios of the refractive index modulations for the different IP concentrations hence indicates where the largest changes in birefringence occur, and where the gain in rotational mobility for the pendant functional groups (chromophores and carbazole groups) is the largest. At a field of 48 V μm$^{-1}$, for the three polymers, the index modulation is raised by a factor of 4 to 6 after addition of 10 wt% IP. Adding another 10 wt% IP (up to 20 wt%) increases the index modulation again, but with a factor of only 1.2 to 1.3. Hence, the highest portion of orientational flexibility is gained after addition of the first 10 wt% IP. After addition of a supplementary 10 wt% IP, the increase in orientational flexibility is considerably smaller. Therefore, the effect of the dilution of the charge transporting groups becomes much larger than the gain in orientational flexibility, and the electrical mobility decreases.

Note that the largest gain in rotational mobility, as determined by the photorefractive experiments, occurs at a temperature below the glass transition temperature ($T_g$) as measured by DSC, where the largest changes would be expected. $T_g$, however, strongly depends on the heating rate.[17] On the time scale of the DSC-measurements, performed at a heating rate of 20 °C min$^{-1}$, the lowering of the $T_g$ below 21 °C (measurement temperature) would indeed provide a substantial increase in rotational mobility that accompanies the phase transition at that scanning rate. When photorefractive measurements are performed, however, the temperature of the samples is allowed to reach a steady state value, which is equivalent to a very slow heating rate. On this longer time scale, the most substantial increase in free volume occurs at lower temperatures than the $T_g$ values obtained from the DSC experiments. This is generally referred to as the time–temperature superposition principle.[17] In addition, our samples were stored for several days at 21 °C. For the samples containing 0 or 10 wt% IP, 21 °C lies below the $T_g$ as determined by DSC (see Table 3). Kovacs has demonstrated that prolonged storage of a polymer sample below $T_g$ resulted in a shrinkage in volume.[17] As a consequence, $T_g$ of those samples is shifted to lower values, due to a change in microstructure, and the gain in rotational mobility at 21 °C after doping with 10 wt% IP is much larger than would be predicted from $T_g$ as measured by DSC measurements.

In summary, addition of 10 wt% IP improves the orientational flexibility of the pendant groups substantially. When the $T_g$ is further lowered by adding another 10 wt% IP, however, this effect is much smaller. This is where the dilution of charge transporter molecules becomes important and shows its effect in a lower photoconductivity and phase shift.

**b. Doping with *N*-ethylcarbazole (ECZ).** Apart from the polymer mixtures with different IP concentrations, we have also prepared a mixture of polymer **1** with 20 wt% of *N*-ethylcarbazole (ECZ). ECZ is a more commonly used plasticizer in photorefractive composites where carbazole is the charge transporting unit. When the glass transition temperature of the latter sample, listed in Table 3, is compared to that of the sample plasticized with 20 wt% IP, it is immediately clear that the IP is a more efficient plasticizer. This explains why the diffraction efficiency of the polymer doped with 20 wt% of ECZ is smaller than in the samples containing 20 wt% of IP, as is shown in Fig. 2c. It is also relevant to analyze the evolution of the phase shifts as ECZ is added as a plasticizer. The phase shift in this sample at 48 V μm$^{-1}$ is presented in Table 3. It is clear that substituting 20 wt% of IP plasticizer with 20 wt% of ECZ enlarges the phase shift substantially, although the $T_g$ of the latter sample is the highest, and lower rotational and charge mobilities would be expected in this sample. Since carbazole is the charge transporting unit in the polymer, however, adding ECZ not only lowers the $T_g$, but also increases the charge transporter

concentration. In this material, there is no dilution of the charge transporter as was discussed for the IP samples, but instead the concentration of charge transporter increases, giving rise to a higher phase shift. When the sample containing 20 wt% of ECZ is compared to the sample with 10 wt% IP, two samples with comparable $T_g$ values, it is again clear that the sample with ECZ shows a larger phase shift. Hence, to obtain large PR phase shifts and two-beam coupling gain coefficients, ECZ clearly is a better plasticizer compared to the inert plasticizer.

The effect of adding ECZ as a plasticizer to polymers **2** and **3** would be more complicated. Whereas for polymer **1** the only charge transporting unit is carbazole, polymers **2** and **3** contain chromophores with an amino donor. Having a lower ionization potential than carbazole, such chromophores can act as a trap at low concentrations, and gradually start participating in the charge transport at higher concentrations.[18,19] Mobility and photoconductivity in those samples are not only affected by $T_g$ and dilution of the charge transporter, but are also strongly influenced by the ratio of carbazole : chromophore.[20]

## Conclusions

In conclusion, we have studied the photorefractive characteristics of three fully functionalized polymethacrylates. We have evaluated two different ways of improving the photorefractive performance by approaching $T_g$. Elevation of the measurement temperature significantly improved the refractive index modulation amplitude, through a larger contribution of birefringence. A strong increase in photoconductivity and phase shift was also observed. When $T_g$ of the samples was lowered by adding an external plasticizer, the refractive index modulation again increased substantially, but photoconductivity and phase shift showed a maximum after addition of 10 wt% of IP plasticizer, due to dilution of the charge transporting groups in the photorefractive mixture. When 20 wt% of the IP plasticizer in polymer **1** was replaced by 20 wt% of ECZ, the phase shift again significantly increased, due to an increase in the charge transport concentration. In polymers **2** and **3**, we have demonstrated a clear correlation between the photorefractive phase shift and the photoconductivity upon raising the measurement temperature or lowering the polymer $T_g$.

## Experimental

### Photorefractive sample preparation

Samples for photorefractive measurements were prepared by dissolving the polymer and the plasticizer in chloroform. 1 wt% TNFM was used as sensitizer for all polymers. After passing this solution through a 0.2 μm PTFE membrane filter, the solvent was allowed to evaporate for 3 hours at 80 °C. The resulting homogeneous mixture was then melted between two ITO-coated glass slides, and the thickness of the samples was controlled by glass spacers of 125 μm diameter.

### Photorefractive characterization

Two-beam coupling experiments and four-wave mixing experiments were done using a set-up described previously.[21] All data were reproducible within 5% of the experimental values. The laser was a diode laser operating at a wavelength of 780 nm. The angle between the two writing beams outside the samples was $(14 \pm 1)^\circ$, and the angle between the bisector and the surface normal was $(50 \pm 2)^\circ$. For the two beam coupling experiments, the two beams were p-polarized, had a power of 2.8 mW each, and were collimated to $(250 \pm 10)$ μm diameter in the sample. The analysis of the data was done using eqn. (3)

$$\Gamma d = \cos\alpha_1 \left( \ln \frac{I_1^t(I_2 \neq 0)}{I_1^t(I_2 = 0)} \right) - \cos\alpha_2 \left( \ln \frac{I_2^t(I_1 \neq 0)}{I_2^t(I_1 = 0)} \right) \quad (3)$$

$I_1^t$ and $I_2^t$ are the transmitted intensities of writing beams 1 and 2. Beam 1 is the beam closest to the surface normal, $\alpha_1$ and $\alpha_2$ are the angles between the writing beams and the surface normal in the sample, $d$ is the sample thickness, and $\Gamma$ is the gain coefficient.

Four-wave mixing experiments were performed using s-polarized writing beams, and a p-polarized probe beam, counter-propagating to writing beam 1. The power of the writing beams was the same as in the two-beam coupling experiments, and the probe beam, collimated to $(150 \pm 10)$ μm, had a power of $(2 \pm 0.1)$ μW. The internal diffraction efficiencies were calculated using the formula

$$\eta = \frac{I_{\text{diff}}}{I_t} \quad (4)$$

where $I_{\text{diff}}$ is the intensity of the light diffracted upon the photorefractive grating, and $I_t$ is the total amount of light transmitted through the sample, that is, the sum of the diffracted and transmitted intensities.


## Acknowledgements

D. V. S. is a research assistant and E. H. is a research associate of the Fund for Scientific Research—Flanders (Belgium) (FWO-V). C. E. obtained a grant from the Flemish Executive (IWT). This research was supported by research grants from the FWO-V (G.0338.98 and S 2/5 – AV. E 8), the University of Leuven (GOA/2000/03), and the Belgian Government (IUAP P4/11).


## References


1 P. Günter and J.-P. Huignard, in *Photorefractive Materials and Their Applications*, Vols I and II, Springer, Berlin, 1988.
2 N. V. Kukhtarev, V. B. Markov, S. G. Odulov, M. S. Soskin and V. L. Vinetskii, *Ferroelectrics*, 1979, **22**, 949.
3 B. Kippelen, S. R. Marder, E. Hendrickx, J. L. Maldonado, G. Guillemet, B. L. Volodin, D. D. Steele, Y. Enami, Sandalphon, Y. J. Yao, J. F. Wang, H. Röckel, L. Erskine and N. Peyghambarian, *Science*, 1998, **279**, 54.
4 E. Hendrickx, B. L. Volodin, D. D. Steele, J. L. Maldonado, J. F. Wang, B. Kippelen and N. Peyghambarian, *Appl. Phys. Lett.*, 1997, **71**, 1159.
5 K. Meerholz, R. Bittner, Y. De Nardin, C. Bräuchle, E. Hendrickx, B. L. Volodin, B. Kippelen and N. Peyghambarian, *Adv. Mater.*, 1997, **9**, 1043.
6 E. Hendrickx, D. Van Steenwinckel, A. Persoons and A. Watanabe, *Macromolecules*, 1999, **32**, 2232.
7 L. Yu, W. K. Chan, Z. Peng and A. Gharavi, *Acc. Chem. Res.*, 1996, **29**, 13.
8 D. Van Steenwinckel, C. Engels, E. Gubbelmans, E. Hendrickx, C. Samyn and A. Persoons, *Macromolecules*, 2000, **33**, 4074.
9 W. E. Moerner, S. M. Silence, F. Hache and G. C. Bjorklund, *J. Opt. Soc. Am. B*, 1994, **11**, 320.
10 H. Ono and N. Kawatsuki, *Opt. Lett.*, 1997, **22**, 1144.
11 H. Kogelnik, *Bell Syst. Techn. J.*, 1969, **48**, 2909.
12 H. Meier, in *Organic Semiconductors*, Verlag Chemie, Weinheim, 1974.
13 N. Tsutsumi, M. Yamamoto and Y. Nishijima, *J. Appl. Phys.*, 1985, **59**, 1557.
14 G. Giro and P. G. Di Marco, *Chem. Phys. Lett.*, 1989, **162**, 221.
15 M. Abkowitz, M. Stolka and M. Morgan, *J. Appl. Phys.*, 1981, **52**, 3453.
16 J. H. Slowik and I. Chen, *J. Appl. Phys.*, 1983, **54**, 4467.
17 G. R. Strobl, in *The Physics of Polymers*, Springer, Berlin, 1997, pp. 217–244.
18 D. Van Steenwinckel, E. Hendrickx, K. Van den Broeck, C. Samyn and A. Persoons, *J. Chem. Phys.*, 2000, **112**, 11030.
19 E. Hendrickx, D. Van Steenwinckel, C. Samyn, D. Beljonne, J.-L. Brédas and A. Persoons, *J. Chem. Phys.*, 2000, **113**, 5439..
20 D. M. Pai, J. F. Yanus and M. Stolka, *J. Phys. Chem.*, 1984, **88**, 4714.
21 B. L. Volodin, Sandalphon, K. Meerholz, B. Kippelen, N. V. Kukhtarev and N. Peyghambarian, *Opt. Eng.*, 1995, **34**, 2213.